Volume 65, Number 1, 2025

ACTA TECHNICA NAPOCENSIS
Electronics and Telecommunications

TEXTURE BASED POLARIMETRIC SYNTHETIC APERTURE RADAR IMAGE CLASSIFICATION USING COVARIANCE MATRICES

Ioana ILEA, Andreia Valentina MICLEA-CECALACA, Mihaela CISLARIU, Raul MALUTAN, George GROSU
Communications Department, Technical University of Cluj-Napoca, Cluj-Napoca, Romania
Ioana.Ilea@com.utcluj.ro, Andreia.Miclea@com.utcluj.ro, Mihaela.Cislariu@com.utcluj.ro, Raul.Malutan@com.utcluj.ro, George.Grosu@campus.utcluj.ro

Abstract: This paper proposes a workflow for polarimetric SAR (PolSAR) image classification based on statistical texture descriptors. The methodology presented in this paper involves spatial interdependence between neighboring pixels as well as multiscale texture representation using wavelet decomposition. The collected features are modeled by zero-mean Multivariate Gaussian Distributions (MGDs). Then, their estimated covariance matrix acts as the texture descriptor and is employed in a k-nearest neighbors (kNN) classifier. Experiments using real PolSAR data validate the proposed approaches' accuracy in land cover categorization, showing their potential for reliable class identification.

Keywords: *PolSAR image, texture, spatial dependence, multiscale analysis, covariance matrix, classification.*

I. INTRODUCTION

Polarimetric Synthetic Aperture Radar (PolSAR) images are radar images captured by Synthetic Aperture Radar (SAR) systems equipped with polarimetric sensors. Unlike conventional SAR, which employs a single polarization (often HH or VV), PolSAR systems can transmit and receive signals in many polarization combinations such as HH, VV, HV, and VH, capturing extensive information on the scattering behavior of different targets in a scene [1].

Numerous relevant characteristics pertaining to vegetation, surface roughness, moisture content, and target type can be extracted due to this comprehensive polarimetric data. Consequently, PolSAR data has been extensively used in a variety of domains, including military surveillance, forestry, agriculture, environmental monitoring and disaster management [2, 3, 4].

Because PolSAR sensors can operate in any weather or at any time of day, they are very useful for continuous monitoring. They are also effective for subsurface and landscape examinations because of their capacity to pierce vegetation layers and expose concealed characteristics beneath the protective canopy.

One of the most important aspects of a PolSAR image is the texture contained in its polarization channels (HH, HV, VV, VH). This texture is an essential component of classification tasks as it offers important spatial and structural information about the scene, being an integral part in differentiating between various forms of land cover. In this paper, textural information is used for land cover classification.

For machine learning algorithms, textural feature extraction can be achieved by means of descriptive statistics-based methods (like gray level co-occurrence matrices, LBPs, etc.) or stochastic based methods, implying the analysis and the statistical characterization of the texture.

Inspired by the work in [5] this paper presents a classification workflow considering statistical approaches. The analysis stage is performed by taking into consideration either the spatial dependency between neighboring pixels, or the multiscale representation of the image. The extracted values are then modeled by Multivariate Gaussian Distributions (MGDs) of zero mean. In the end, the covariance matrix characterizing the distribution is estimated and used as the final texture descriptor for land cover classification.

The paper is organized as follows: in the context of polarimetric SAR remote sensing, Section II introduces our proposed methodology. With an emphasis on experimental validation, Section III presents the classification results derived from actual PolSAR imagery, where textural information is extracted from several polarimetric channels. Finally, Section IV summarizes the important findings and considers possible future research topics.

II. PROPOSED METHOD

The proposed workflow for this study, which focuses on polarimetric SAR image classification, is shown in Figure 1. The polarization channels HH, HV and VV are independently pre-processed and used as inputs for texture analysis and statistical modelization by means of a zero-mean Multivariate Gaussian Distribution. Starting from this probabilistic model, its parameter represented by the covariance matrix is estimated and employed as the final feature vector for classification.

A. Data structure and pre-processing

Polarization in Polarimetric Synthetic Aperture Radar imaging refers to the orientation of electromagnetic waves emitted and received by the radar system with respect to the Earth's surface. PolSAR systems are equipped with antennas that can operate in several polarization modes, allowing them to send and receive signals in a variety of configurations, including horizontal-horizontal (HH),

Manuscript received April 15, 2025; revised June 26, 2025

horizontal-vertical (HV), vertical-horizontal (VH), and

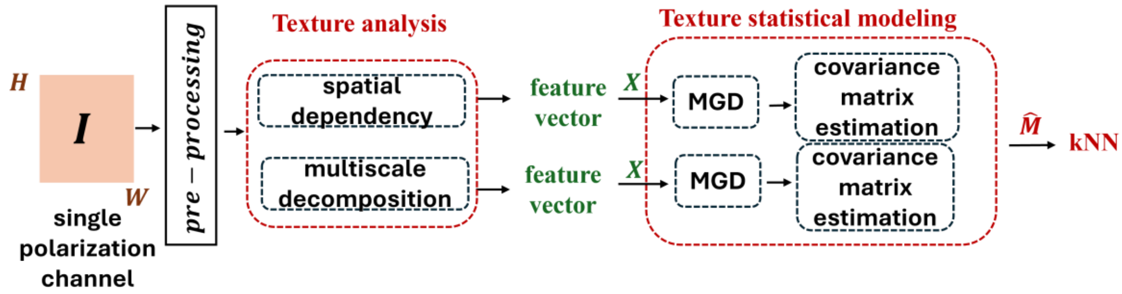

Figure 1. Polarimetric Synthetic Aperture Radar image classification workflow.

vertical-vertical (VV). When electromagnetic pulses are transmitted toward the Earth's surface during acquisition, they disperse when they come into contact with objects in the scene. The backscattered signals are captured by the radar revealing details on the structural and physical characteristics of the target [3]. In polarimetric SAR imaging, the interaction between the incident and scattered electromagnetic waves can be represented using the scattering matrix S, as illustrated in equation (1):

$$\begin{bmatrix} E_h^s \\ E_v^s \end{bmatrix} = \frac{e^{-jkr}}{r} \begin{bmatrix} S_{hh} & S_{hv} \\ S_{vh} & S_{vv} \end{bmatrix} \begin{bmatrix} E_h^i \\ E_v^i \end{bmatrix} = S \begin{bmatrix} E_h^i \\ E_v^i \end{bmatrix} \quad (1)$$

The incident waves, polarized in the horizontal (E_h^i) and vertical (E_v^i) directions, illuminate the target, which then reflects the energy back toward the radar as scattered waves (E_h^s and E_v^s). This scattering process is influenced by the target's physical characteristics and occurs over a distance r between the radar and the target in the scene. The scattered field is expressed as a linear combination of the incident field components, weighted by the complex-valued elements of the scattering matrix S, which includes S_{hh}, S_{hv}, S_{vh} and S_{vv}. These matrix elements describe how the target reflects energy between different polarization combinations. The relationship is scaled by a complex exponential factor e^{-jkr}, accounting for wave propagation over distance and phase shift [2].

The diagonal elements of the scattering matrix are typically thought to be comparable when the transmitter and receiver are placed together, suggesting that the information carried by the HV and VH polarization channels is the same. PolSAR imaging provides more comprehensive knowledge of surface scattering mechanisms and structural features by combining data from several polarization states. The accuracy of classification tasks can be influenced by this multi-polarization study. The diagonal and vertical scattering coefficients, HH, VH, and VV channels, are subjected to a logarithmic transformation, as indicated by the equation (2):

$$\begin{aligned} I_{hh} &= 10log[Re^2(S_{hh}) + Im^2(S_{hh})] \\ I_{hv} &= 10log[Re^2(S_{hv}) + Im^2(S_{hv})] \quad (2) \\ I_{vv} &= 10log[Re^2(S_{vv}) + Im^2(S_{vv})] \end{aligned}$$

B. Feature extraction

In this paper, the feature considered for land cover classification based on PolSAR images is the texture. The characteristics of different surfaces are described by means of covariance matrices, which have proven their power of discrimination in various applications, including PolSAR image classification [5].

Covariance matrix extraction consists in two steps, as suggested in [5], namely texture analysis and texture statistical modeling, that are detailed further.

i. Texture analysis

Starting from real-valued individual polarimetric channels, texture analysis is performed by two methods: first, the spatial dependence between neighboring pixels is considered, and second, the multiscale decomposition is taken into account.

Let consider a single polarization image I, of size $W \times H$, containing N pixels, with $N = W \times H$.

In the case of spatial dependence modelization, for each pixel in the image, an $w \times w$ sliding window is applied, capturing the spatial information. Next, the window's elements are concatenated into a vector and the set of all vectors obtained from the entire image will describe its textural content.

For the second approach, textural information is captured by multiscale analysis. The input image is decomposed using wavelet filters, resulting in a set of B subbands. For each pixel, the decomposition coefficients in the B subbands are organized in a vector and the set of all vectors will characterize the image.

In the end, for both methods, an image is represented by a set of N m-dimensional vectors, defined in equation (3):

$$\boldsymbol{X} = \{\boldsymbol{x}_1, \cdots, \boldsymbol{x}_N\}, \quad (3)$$

where m is the number of pixels in the considered neighborhood, or the number of subbands used for the wavelet decomposition, and N the number of pixels in the input image I.

ii. Texture statistical modeling

Once extracted, the m-dimensional vectors are modeled by means of statistical tools. In this work, they are considered to be independent and identically distributed random vectors issued from a zero-mean Multivariate Gaussian Distribution, described by the probability density function in equation (4):

$$p(\boldsymbol{x}|\boldsymbol{M}) = \frac{1}{\sqrt{(2\pi)^m|\boldsymbol{M}|}} \exp\left(-\frac{1}{2}\boldsymbol{x}^T\boldsymbol{M}^{-1}\boldsymbol{x}\right), \quad (4)$$

where $\boldsymbol{M}$ is the covariance matrix.

The final descriptor of each image will be represented by the $m \times m$ estimated covariance matrix, denoted by $\widehat{\boldsymbol{M}}$. Based on the previously extracted vectors, the estimation will be performed by using the sample covariance estimator, as defined in equation (5):

$$\widehat{\boldsymbol{M}} = \frac{1}{N}\sum_{i=1}^{N} \boldsymbol{x}_i \boldsymbol{x}_i^T, \tag{5}$$

where $(\cdot)^T$ denotes the transpose operator.

C. Classification

In order to perform the classification task using the k-nearest neighbor algorithm (kNN), a similarity measure between two images is needed. The final descriptor of an image being the estimated covariance matrix, the similarity measure has to take into account the properties of these matrices. Therefore, the Kullback-Leibler divergence has been considered. For two covariance matrices, denoted by $\widehat{\boldsymbol{M}}_1$ and $\widehat{\boldsymbol{M}}_2$, the divergence is defined in equation (6) [6]:

$$KL(\widehat{\boldsymbol{M}}_1, \widehat{\boldsymbol{M}}_2) = \frac{1}{2}\left[tr(\widehat{\boldsymbol{M}}_2^{-1}\widehat{\boldsymbol{M}}_1) - m - \ln\frac{|\widehat{\boldsymbol{M}}_1|}{|\widehat{\boldsymbol{M}}_2|}\right], \tag{6}$$

where $tr(\cdot)$ is the trace operator and m is the dimension of the vector space. In practice, the symmetrical Kullback-Leibler divergence is employed, which is given in equation (7):

$$SKL(\widehat{\boldsymbol{M}}_1, \widehat{\boldsymbol{M}}_2) = KL(\widehat{\boldsymbol{M}}_1, \widehat{\boldsymbol{M}}_2) + KL(\widehat{\boldsymbol{M}}_2, \widehat{\boldsymbol{M}}_1). \tag{7}$$

III. EXPERIMENTAL RESULTS

A. Dataset

To test the proposed algorithms, the L-band Oberpfaffenhofen PolSAR image was considered [7]. The image was acquired in the Oberpfaffenhofen region in Germany. The image has a spatial resolution of 3 meters and contains three major land cover classes: built-up areas, forest lands and open areas. The three polarimetric channels, HH, HV, and VV, employed in this paper, are shown in Figure 2.(a-c). Based on the information given in [8], the manually labeled ground truth map illustrated in Figure 2.d was obtained. A set of 196 nonoverlapping images of 64×64 pixels were extracted and divided, as follows: 21 images for the built-up areas class, 125 images for the forest lands class and 50 images for the open areas class. The labeled database was further used for land cover classification, to validate the proposed algorithms.

B. Results

The performed tests have multiple purposes. First, the most appropriate approach for land cover classification needs to be identified, which in this case is either the spatial dependence between neighboring pixels, or the multiscale decomposition. Second, the polarization channel that contains the relevant textural information for classification has to be detected. Third, the information extracted from the three polarimetric channels is merged, and the decision level fusion based classification algorithm introduced in [3] is analyzed. In this case, the classification is performed on all the available polarization channels and the final result, for each image, is given by the class which occurs more often among the studied polarizations. To perform the classification using the kNN algorithm, the dataset has been randomly split 100 times into testing and training sets, each of them containing 50% of the images in each class. Different values for k, the number of neighbors involved in the classifier, have been evaluated and the classification results have been quantified using the overall accuracy. Its mean value and standard deviation computed for the 100 iterations are reported further.

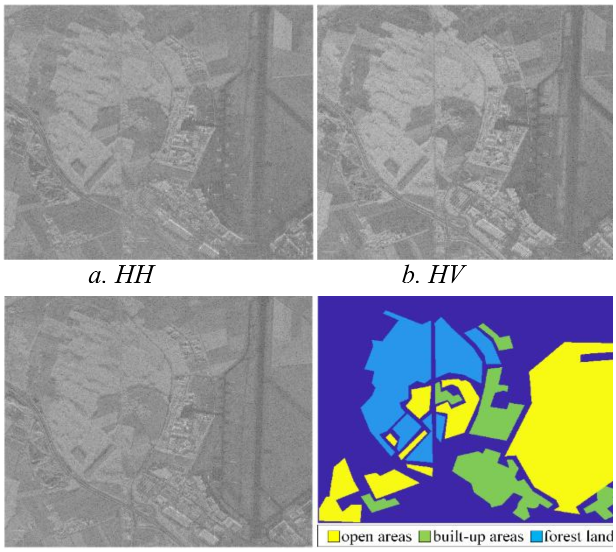

a. HH *b. HV*

c. VV *d. Ground truth*

Figure 2. Oberpfaffenhofen PolSAR image for HH, HV and VV polarizations, with the corresponding ground-truth class labels.

The algorithms have been implemented in MATLAB R2021a, and the tests have been carried out on a computer with an Intel 11th Gen Core i7-1165G7 Processor running at 2.8MHz using 16GB of RAM.

i. Texture analysis by spatial dependence modelization

For the first experiment, the correlation between neighboring pixels has been evaluated. Therefore, the content of the input images has been analyzed by using a sliding window of variable size. Tests have been performed to study the importance of the window size, w, for texture modelization and the results are presented in Table 1, for w equaling 3, 5 and 7. The values have been chosen with respect to the resolution and the size of the input images.

Even though the amount of information that is used to describe the texture depends on the number of neighboring pixels, the classification results are slightly influenced by this parameter, the accuracy being around 99%. On the other hand, the running time of the classification algorithm is strongly influenced by the window size, which gives the size of the vector space $m = w \times w$, and therefore, the size $m \times m$ of the covariance matrices. More precisely, for $w = 3$, the running time was around 57s, while for $w = 7$ it increases to 1100s.

In addition, it can be noticed that HH polarimetric channel is slightly better for texture characterization, while the majority voting strategy brings no improvement. The best classification accuracy ($99.64\% \pm 0.52\%$) has been obtained on HH polarimetric channel, when sliding windows of 7×7 pixels have been employed.

ii. Texture analysis by multiscale decomposition

For the second experiment, the texture has been analyzed in the time-frequency domain, by means of

Table 1. Influence on the classification accuracy of the sliding window size for spatial dependence modelization.

Window size (w)	HH	HV	VV	Majority Voting
$\mathbf{3 \times 3}$	99.07 ± 0.77	98.46 ± 0.84	98.41 ± 0.90	98.89 ± 0.70
$\mathbf{5 \times 5}$	99.54 ± 0.56	99.46 ± 0.58	99.04 ± 0.93	99.55 ± 0.55
$\mathbf{7 \times 7}$	$\mathbf{99.64 \pm 0.52}$	99.66 ± 0.36	98.88 ± 0.98	$\mathbf{99.68 \pm 0.48}$

Table 2. Influence on classification accuracy of the number of decomposition levels and wavelet subbands for multiscale decompositions.

Number of scales	Subbands	HH	HV	VV	Majority Voting
1	**H/V/D**	64.80 ± 3.86	55.74 ± 4.20	62.94 ± 3.64	65.68 ± 3.21
	A/H/V/D	93.66 ± 1.53	93.23 ± 2.33	93.48 ± 1.99	94.68 ± 1.56
2	**H/V/D**	86.07 ± 2.86	77.64 ± 3.30	79.61 ± 2.64	86.57 ± 2.76
	A/H/V/D	$\mathbf{98.55 \pm 0.92}$	98.38 ± 0.91	97.88 ± 1.04	$\mathbf{98.70 \pm 0.81}$

wavelet filtering. To compute the covariance matrix among wavelet subbands, the Daubechies db4 stationary wavelet transform has been considered, which discards the downsampling and upsampling operations from wavelet filter banks. The filtering process has been iteratively repeated to extract the textural information available at different scales. In this paper one and two levels of decomposition have been used, and the results are presented in Table 2.

Moreover, the influence of the employed wavelet subbands is discussed. First, tests have been conducted for covariance matrices computed based on horizontal (H), vertical (V) and diagonal (D) details, denoted further by H/V/D. Next, they have been combined with the approximation (A) coefficients, approach identified as A/H/V/D. In practice, the number of decomposition levels and subbands influence the size of the vector space m, thus the size of the covariance matrix. The obtained classification results are also given in Table 2.

The tests have shown that by expending the depth of the multiscale decomposition, in this case the number of decomposition levels from one to two levels, the classification accuracy increases by 16% up to 21%, when H/V/D subbands have been considered. For the A/H/V/D approach, when the approximation coefficients have been added, the accuracy increases by 5%.

If the number of decomposition levels is fixed, the classification accuracy growth is even more important (between 12.5% and 37.5%) when comparing A/H/V/D with H/V/D approach. The results emphasize that textural information is well described by the approximation coefficients.

The best classification accuracy ($98.55\% \pm 0.92\%$) has been obtained on HH polarimetric channel, when four subbands (A/H/V/D) and two decomposition levels have been used. Depending on the combined parameters, majority voting strategy brings minor improvements (about 0.5%) with respect to the classification accuracy obtained on HH polarimetric channel.

Overall, by analyzing the entire set of results, it can be noticed that spatial modelisation gives the highest accuracy, providing enough information for classification.

IV. CONCLUSIONS

This paper introduces a classification workflow for PolSAR image classification using texture features. Two descriptors based on covariance matrices have been proposed and integrated into the kNN classifier along with the symmetrical Kullback-Leibler divergence. First, the spatial dependency between neighboring pixels has been modeled and then, the wavelet decomposition has been employed, for multiscale characterization of texture. The methods have been evaluated for land cover classification, showing their importance for class identification.

Further works will concern the generalization of the proposed algorithm for pixel-based classification used for image segmentation.

ACKNOWLEDGEMENTS

This work was supported by the “Algoritmi de clasificare în spațiul Riemannian pentru imagini polarimetrice SAR” grant funded by the National Grant Competition - GNaC ARUT 2023.

REFERENCES

[1] Z. Wang, X. Zeng, Z. Yan, J. Kang, and X. Sun, “AIR PolSAR-Seg: A Large-Scale Data Set for Terrain Segmentation in Complex-Scene PolSAR Images,” IEEE Journal of Selected Topics in Applied Earth Observations and Remote Sensing, vol. 15, pp. 3830-3841, 2022.
[2] I. Hajnsek and Y. L. Desnos,” Polarimetric Synthetic Aperture Radar: Principles and Application.” Springer Nature, 2021.
[3] A. Miclea, I. Ilea, and R. Terebes. “Extended Local Binary Patterns-Based Polarimetric Synthetic Aperture Radar Image Classification.” Acta Technica Napocensis, vol. 64, no. 1, pp. 20-25, 2024.
[4] H. Wang, C. Xing, J. Yin, J. Yang. Land Cover Classification for Polarimetric SAR Images Based on Vision Transformer. Remote Sensing, vol. 14, no. 18, pp. 4656, 2022.
[5] I. Ilea, L. Bombrun, C. Germain, I. Champion, R. Terebes, and M. Borda, “Statistical hypothesis test for maritime pine forest SAR images classification based on the geodesic distance,” in 2015 IEEE International Geoscience and Remote Sensing Symposium, pp. 3215-3218, 2015.
[6] S. Kullback, R. A. Leibler, “On Information and Sufficiency.” The Annals of Mathematical Statistics, vol. 22, no. 1, 1951.
[7] PolSARpro. Polarimetric SAR Data Processing and Educational Tool.
[8] Y. Cao, Y. Wu, P. Zhang, W. Liang, M. Li, “Pixel-Wise PolSAR Image Classification via a Novel Complex-Valued Deep Fully Convolutional Network.” Remote Sensing, vol. 11, 2019.